Measurement 174 (2021) 109037

Contents lists available at ScienceDirect

Measurement

journal homepage: www.elsevier.com/locate/measurement

Metrological comparison of LiDAR and photogrammetric systems for deformation monitoring of aerospace parts

E. Aldao [a], H. González-Jorge [a,*], J.A. Pérez [b]

[a] School of Aerospace Engineering, University of Vigo, Spain
[b] School of Industrial Engineering, University of Vigo, Spain

ARTICLE INFO

Keywords:
LiDAR
Metrology
Photogrammetry
Aerospace industry

ABSTRACT

The inspection of airframes and aerodynamic surfaces is a very important task in aeronautical maintenance. Traditionally, this labor has always been carried out by maintenance personnel, who manually checked all the parts of the fuselage, which is a great cost for the airlines. This article evaluates the feasibility of implementing low cost portable 3D scanning systems to perform these inspection tasks easily and accurately. A metrological comparison among a LIDAR Kinect One sensor, a single digital camera Sony Alpha 6000 using photogrammetry software and a stereoscopic ZED camera was performed. Their behavior is characterized as well as their main sources of error to determine which technology is the most suitable for inspecting aeronautical surfaces. Kinect LIDAR sensor shows the most promising results and opens the possibility to apply this technology to aircraft maintenance tasks in future.

1. Introduction

Preventive maintenance is an essential task to avoid any type of failure and ensure the correct operation of any machine or structure. In the aerospace industry this factor is truly critical, since some flaws can have catastrophic consequences. Defects such as deformations and dents can be a risk as they modify the tension distribution concentrating the stresses in certain areas which may help crack propagation [1]. Certain areas such as propellers, nose cone of fuselage and the leading edge of wings are susceptible to bend damage due to bird strikes, meteorological factors such as lightning strikes or hail impacts [2–4]. Therefore, regular inspections must be carried out to check the magnitude of the damage and assure the aircraft preserves its airworthiness.

According to the FAA regulations, all commercial aircraft must pass an inspection every 100 h of flight [5]. Traditionally, visual inspection has always been the most common technique. Qualified personnel check all surfaces to detect tears, distortion, deterioration, dents, corrosion and other issues. Generally, the lack of contrast and reflectance in most of the surfaces makes it difficult to detect these defects and special equipment such as flashlights and mirrors are required. Besides, visual acuity is a very important factor and maintenance staff must pass visual acuity tests. In fact, the age of the inspectors is quite a relevant factor, since the detection capacity decreases with age [6,7].

Due to the large size of the commercial airplanes, to inspect some areas such as the upper parts of the fuselage and the empennage, certain types of structures such as ladders, adjustable platforms and cranes are required, which increases the inspection time sometimes up to 24 h. For this reason, in the recent years, some companies as Airbus have been developing an inspection system based on UAV and digital cameras which allows to reduce the influence of the human factor and enables to perform an inspection in about three hours. These pictures are processed and sent to a ground control station, where the maintenance personnel revise all of them to determine if there is any damage [8].

However, UAV technology still requires qualified staff to check the images manually. For this reason, in this article we will study the possibility of implementing a system of 3D scanners embedded in UAV to perform these inspection tasks autonomously. These sensors would obtain a 3D point cloud of the different parts of the aircraft, which would allow to determine the existence of deformations in the surfaces comparing the measurements with a CAD reference model. The main advantage of this system is that a geometric disparity map would be obtained, showing the differences between the reference CAD and the inspection point cloud. This technique is also commonly used in the manufacturing industry to ensure the quality of the products [9].

Nowadays, most of the commercial airplanes use composite materials in their airframes as they are lighter than traditional aluminum

* Corresponding author.
E-mail address: higiniog@uvigo.es (H. González-Jorge).

https://doi.org/10.1016/j.measurement.2021.109037
Received 10 September 2020; Received in revised form 21 November 2020; Accepted 12 January 2021
Available online 22 January 2021

alloys. Nevertheless, for these materials it is more difficult to predict their behavior under impacts, since several factors such as delamination, matrix cracking and fiber breakage intervene in its impact energy absorption mechanism [10]. According to [11], the first damage mechanism is often due to the initialization of a delamination area, which increases its size and activates other damage propagation mechanisms. It has been proved that a dent with a depth of 1.3 mm can delaminate composite material skins creating a weakened area with worse mechanical properties [12]. Therefore, it is important to ensure a correct maintenance plan to avoid this type of damage and ensure the safety of the structure. In order to implement any type of 3D scanner, it is essential to perform a metrological test, ensuring the accomplishment of measurement tolerance and the detection of these defects.

LIDAR sensors and photogrammetry cameras are widely used in aerial 3D mapping. They are relatively inexpensive, light, and able to provide high resolution reconstructions [13]. In this article, the possibility of implementing one of these technologies for aerospace maintenance will be studied using low cost devices: a mirrorless camera Sony Alpha 6000 along with photogrammetry software, a stereoscopic camera ZED and the LIDAR sensor Microsoft Kinect One.

This first section shows a brief introduction to the problem and the description of the concept to be evaluated. To perform this task, in this work several metrological comparisons will be performed to determine the precision and accuracy of the sensors. Various types of surfaces will be scanned to determine the performance of the sensors in different situations as well as to determine the main sources of error of the compared technologies. The manuscript is organized as follows: Section 2 describes the hardware and the characteristics of the different physical artefacts, as well as the measurement procedures and the post-processing methods of the point clouds. Section 3 depicts the results and their discussion. Finally, Section 4 exhibits the obtained conclusions.

2. Materials and methods

2.1. Materials

2.1.1. Laser scanning and photogrammetric systems under study

2.1.1.1. Kinect One. Kinect One is a sensor released along with the console Microsoft Xbox One. The main application of this device was to allow users to interact with the console and play games using gestures and voice commands. Nevertheless, thanks to the Kinect SDK and the libraries Libfreenect2, developers have found other uses of the device such as 3D scanning or movement tracking. It is compatible with Microsoft Windows and Linux using a special power adapter. It combines an RGB video-camera with a Time of Flight (ToF) sensor to obtain 3D images of a scene. The ToF sensor consists of a light emitter, which sends modulated infrared pulses, and a CMOS sensor, which collects the reflected light to determine the distance as a function of the time of flight. It has implemented a clock signal which synchronizes the pulse emission with the reception to determine the quantity of light received in the different parts of the pulse. Using a quantum-efficiency-modulation (QEM) algorithm, it computes the phase shift and distance integrating the received light during different periods of time [14].

2.1.1.2. ZED stereo camera. ZED is a stereo camera released by the company Stereolabs. It was mainly designed for robotic and autonomous navigation applications. It can provide real time tridimensional images combining the information from two cameras. The working principle of the stereoscopic camera is very similar to the human vision. It combines the information from two cameras separated a distance B (commonly named as baseline) to determine the disparity between the two images. Distance can be computed using triangulations and conic projections of the image with the PinHole Camera Model [15]. Stereolabs released a Software Development Kit which allows to create specific applications for this sensor. An Nvidia GPU compatible with CUDA is required to use this software to accelerate the computing process. However, Nvidia has released a series of small single-board computers (Nvidia Jetson) which are able to run the ZED SDK, facilitating the implementation in mobility applications such as UAVs or small robots.

2.1.1.3. Sony Alpha 6000 camera. In addition to the first two sensors, a Sony Alpha 6000 mirrorless camera was also used, along with a Sony EPZ lens with a variable focal length between 16 and 50 mm. These systems are selected because laboratory availability. Unlike the Kinect and ZED, the camera cannot obtain measurements in real time. In fact, its main application is not for 3D scanning purposes, but thanks to a postprocessing process of the captured images with photogrammetry software, it is possible to obtain point clouds from scenes. This software searches for identifiable features in the different pictures and stablishes a set of triangulations to estimate the pose of the camera in every image with respect to the reference elements. It is a complex and computationally expensive process because the software does not initially know the position of the cameras [16]. A modern computer can take several hours to finish processing. On the contrary, this type of post-processing allows to obtain models of higher resolution than stereoscopic vision since it does not need to perform calculations in real time [17]. No commercial photogrammetry software is available on the laboratory, so Meshroom free software is used to obtain three-dimensional reconstructions from a series of photographs. This program was used for all tests performed, although there are many other alternatives available. Data acquisition was done using the maximum resolution of the camera (24.3 MP) and a focal length fixed at 50 mm. Distances from camera to samples range around 1–1.5 m. Convergence photogrammetry is used as acquisition technique. Camera calibration is done previously to data acquisition. Although self-calibration methods show more accurate results [18,19], previous calibration methodology was selected because the study was linked with an engineering student training and it seems more easily understandable. Control points to apply scale are manually marked using singular points of the scene.

2.1.2. Metrological artefacts

This section will describe the equipment that was used to complete the metrological evaluation of the systems previously described.

2.1.2.1. RMS deviation from ideal plane. A flat chessboard and a white painted aluminum plate were used to check the noise of the sensors scanning flat surfaces. They can be considered as completely flat surfaces. They have a smooth finish and very little roughness. Surface imperfections due to manufacturing tolerances are neglected with respect to the sensor accuracy range (see Figs. 1–4).

2.1.2.2. Depth pattern. Rectangular cutouts with a square hole of six centimeters side in the central part were made from aluminum plates. By stacking several cutouts, a pattern of levels of depth can be formed. Different numbers of cutouts were placed at each vertex to form different levels of width. The depth in the central hole of each cutout was measured with a Magnusson Vernier Caliper, a device with a resolution of 0.02 mm, obtaining the results of Fig. 5 (see Figs. 6 and 7).

Fig. 1. Laser scanner Kinect One.

Fig. 2. Stereo camera ZED.

Fig. 3. Digital camera Sony Alpha 6000.

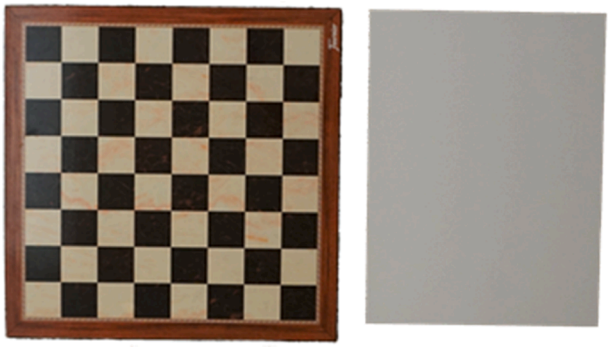

Fig. 4. Chessboard (left) and aluminum plate (right).

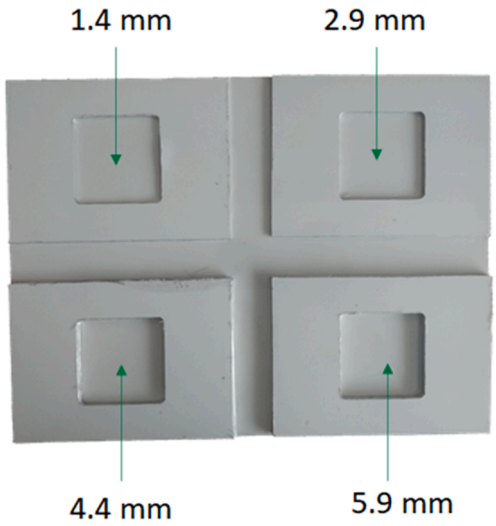

Fig. 5. Depth pattern.

2.1.2.3. Dent detection test. An aluminum plate was placed on the top of the hollow rectangular cutouts from the previous test. The plate was hit in the part of the gaps to produce dents of different depths, as shown in the attached image. Finally, the depth in the central part of the dents was measured with the Magnusson Vernier Caliper.

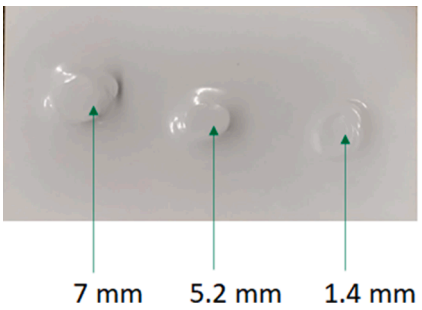

Fig. 6. Dented aluminum plate.

Fig. 7. Scanned airplane propeller.

2.1.2.4. Aircraft blade scanning test. A blade from a Hartzell HC-B3TN-5E propeller was scanned. This component has a length of 1.35 m and comes from a Honeywell TPE331 engine, with a power of up to 665 hp. In addition, to being a direct test of an aeronautical element, it is an interesting test since it allows to evaluate the behavior of the sensors on surfaces with complex curvatures.

In this test, a CMM machine Altera 15.7.6 was used, with which a point cloud was obtained from the surface of the plane propeller. The equipment has a 19 mm calibration sphere, with calibration certificate and has been subjected to precision tests according to ISO 10360-4: 2000 standards [20]. The probe precision in MPE contact mode is 1.7 μm, which is considerably superior to the sensors to be tested, so this point cloud will be used as a reference model to determine some metrological characteristics of the sensors under study. Camio 8.4 was used to perform the measurements with this device.

2.2. Methods

2.2.1. Calibration procedures

All devices were calibrated prior to performing the scan tests. Due to the geometry of the lenses and faults in the manufacturing process, the cameras present a certain distortion in the images, which causes errors in the reconstruction by photogrammetry [21]. These imperfections are inevitable and practically all the cameras present some distortion. However, there are calibration algorithms that digitally correct images through a fit with a polynomial expression. The correction functions can be calibrated through photographs taken by the sensors. One of the most common procedures is to obtain images of a chessboard and compare them with a reference model without distortion. In this way, the parameters of the distortion function are estimated to minimize the difference between the images and the reference model.

The distortion function depends on the camera lens. Therefore, it is important to calibrate the camera with the parameters to be used in the tests. According to [22], the distortion function varies with the focal length and the focus plane of the camera. Generally, in aerial photogrammetry the focus is kept fixed, and a long focal length is used to minimize the distortion that occurs in the images. However, for short distance photogrammetry, this is not feasible as the effects of blur when

moving objects from the focus plane are more noticeable. For all tests performed with the Sony Alpha the maximum focal length of the lens was used to minimize distortion. In addition, the camera was calibrated at a distance of 1 m, a value similar to that used in all tests.

For the calibration, the Matlab camera calibration libraries were used. Photographs of the chessboard shown above were taken and the distortion parameters were obtained with Matlab. For the ZED, a similar procedure was followed, but the ZED SDK calibration suite was used, which allows to obtain the parameters of the two cameras simultaneously. The Kinect's sensors also experience this distortion. Although this is not so important because the device does not perform image triangulations to obtain depth measurements. Therefore, Microsoft's default calibration was used.

On the other hand, it is important to consider that LIDAR sensors are sensitive to temperature variations. The operation of the light receivers of the CMOS sensor varies with temperature and drift in measurements may occur [23,24]. The Kinect One works at a voltage of 12 V and generates considerable heat that can disturb the measurements. It presents a fan to regulate the temperature, but it takes some time to reach thermal equilibrium. In fact, it is important to set a warm-up period (around 30 min according to the references) before using the sensor so that the device reaches thermal equilibrium and the measurements stabilize accurately.

2.2.2. Metrological tests

2.2.2.1. RMS deviation from ideal plane. A chessboard and a white painted aluminum plate were scanned using the three devices. Both the Kinect and the ZED were placed perpendicularly to the surfaces to be scanned at 1-meter distance. With the fixed sensors, the point cloud of the aluminum plate and the chessboard were obtained. For the Sony Alpha camera, several photos were taken from different positions varying the angle to the surface to be scanned. The images were loaded in Meshroom to obtain a tridimensional model.

Once the point clouds were obtained, they were processed with CloudCompare. All of them were approximated with a plane adjusted by least squares. The main quadratic deviation (RMS) from the points to the ideal plane was computed using CloudCompare tools.

2.2.2.2. Depth pattern. The scanning procedures in this test were the same as in the previous one. The hollow aluminum cutouts were trimmed and a plane was adjusted to the central square hole using least-squares fit. The region near the edges between the hole and the outer rectangular frame of the cutout was removed to avoid the burr of this area. Another plane was fitted to the outside of the square hole. Once the planes were adjusted, the perpendicular distance between them was computed to obtain the depth measurement. This value was compared with the measure of the Magnusson Vernier Caliper. This procedure was performed for the four rectangular cutouts to obtain the relative error in the measured distances. CloudCompare was used to perform all of these operations.

2.2.2.3. Dent detection test. The deformed aluminum plate was scanned with all the sensors. Then, the resulting point cloud was fitted to a plane using CloudCompare. With the 2.5D volume tool, the distance from the point cloud to the plane was calculated. It generates a 2.5D mesh of the point cloud and computes the volume between the plane and the obtained mesh. Then, it obtains the distance, as a function of the volume and cell width. Finally, it interpolates the results of the cells to obtain the depth maps shown in the results section.

2.2.2.4. Aircraft propeller scanning test. In this final test, an aircraft propeller was scanned with the sensors and the measurements were compared with the values provided by the CMM. A dataset of 331 points of the geometry of the propeller was obtained using probe scanning. For the Sony Alpha camera, images were taken from different angles covering the entire surface of the blade, from a distance of approximately one meter. For the ZED and Kinect sensors, the different parts of the surface were focused moving the sensors during the scanning process to reconstruct the scene. The SDKs of both devices have point cloud fusion applications, which determine the position of the cameras and perform the point cloud registration during the movement of the sensor to create the complete reconstruction of the scene.

The measurements of the different sensors were compared with CMM point cloud. Firstly, the clouds were aligned by taking pairs of reference points in both of them. Secondly, to improve the registration, an iterative closest point (ICP) algorithm was used to minimize the distance between both point clouds. Finally, the 2.5 vol was computed between both point clouds. Instead of using the plane adjusted with least squares, another 2.5D mesh was generated using the CMM values to compute the volume among the two clouds.

3. Results and discussion

Fig. 8 shows the root mean square (RMS) deviation from an ideal plane fitted from the point clouds obtained for the chessboard and the aluminum plate. The results show a very different trend among the Kinect and the other sensors. The noise on the generated point cloud for the ZED and the Sony Alpha is higher on the aluminum plate than in the chessboard. This is due to the way the sensors calculate depth, based on image processing. They use feature detection and matching algorithms for localization and mapping, which identify references in the different pictures to establish triangulations [25]. One example of feature detectors is the scale-invariant feature transform (SIFT), which uses the maxima from a difference-of-Gaussians (DOG) pyramid as features. The first step in SIFT is finding a dominant gradient direction. To make it rotation-invariant, the descriptor is rotated to fit this orientation. Another common feature detector is the SURF (speeded-up robust features). In SURF, the DOG is replaced with a Hessian matrix-based blob detector. Also, instead of evaluating the gradient histograms, SURF computes for the sums of gradient components and the sums of their absolute values. Its usage of integral images allows the features to be detected extremely quickly with high detection rate.

However, these methods rely on the visual properties of the surfaces [26,27]. Patterned surfaces, such as the chessboard are easily recognizable as there are great contrasts between the different colors of the images. Other surfaces, such as the white aluminum plate, present problems as the surface is completely homogeneous and the software cannot correctly identify different patterns.

There are also some differences in the performance between the ZED and the Camera Sony Alpha 6000. The latter, obtains a remarkable precision for the chessboard, with a RMS around 0.2 mm, and an RMS around 1.3 mm for the aluminum plate. The RMS of the ZED was much higher in both surfaces. There are several reasons that explain these results:

ZED lenses have a very short focal length of only 2.65 mm, according to manufacturer specifications, which considerably increases image distortion and reconstruction errors. Stereolabs chose to use lenses with this focal length as it provides a very wide field of view. It is very useful for navigation and orientation applications, but worsens sensor accuracy. Additionally, single camera photogrammetry uses multiple images to obtain depth, which helps to reduce the influence of distortion on reconstruction. Since the ZED is not intended to be used for scanning at short distances, it does not have an autofocus system. This is beneficial as it is not necessary to calibrate the sensor for different distances, but it does result in a loss of sharpness in images.

Another quite relevant factor is the resolution of the sensor. The Sony Alpha photos have a considerably higher resolution than the ZED. The latter is limited by the computational cost of real-time photogrammetry. To obtain point clouds in real time, a great computing power is required as well as great data transfer capacity. The ZED records video in

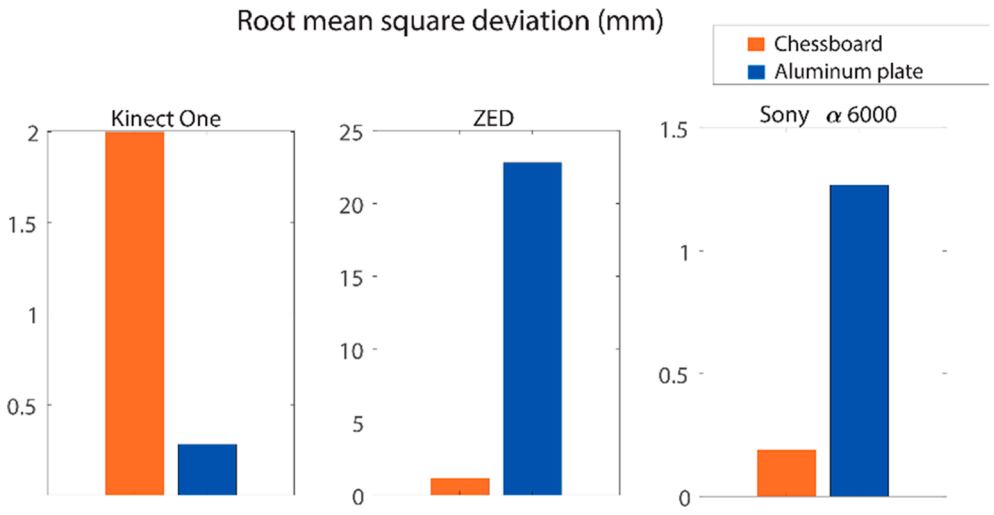

Fig. 8. Root mean square deviation.

resolutions up to 2.2 k from its two cameras, a large amount of information that must be sent and processed. If it were decided to increase the resolution, it would substantially increase the necessary computing power as well as the data transmission speed, which would not be feasible to execute on a single board computer with current technology.

On the other hand, the RMS in the chessboard is better for the Kinect. LIDAR technology seems to be an excellent option to scan flat and homogeneous surfaces such as also the aluminum plate. Nevertheless, errors increase when scanning surfaces with variable reflectivity (Fig. 9).

The algorithm used by the Kinect One to calculate the distance depends on the amount of light received. Surfaces with varying reflectivity can present problems for this sensor, as the amount of reflected light reaching the sensor varies and errors occur in the calculation of the phase shift of the modulated signal. Reflectivity is a property that depends on multiple factors, but in general darker objects tend to reflect less light. In the performed tests, the black squares of the chessboard appeared slightly closer than the white ones due to the difference in reflectivity, which increased the RMS.

Fig. 10 represents the errors of the sensors expressed as a percentage on the measurement of the depth pattern, measuring the distance between the square hole and the rectangular outer frame. As it was expected, the ZED is the worst of the three sensors, with errors greater than 100%. Due to the high noise of the point cloud, in some of the measurements, the central hole appears closer to the sensor than the outer frame, measuring negative depths. The results for the ZED in this test are poor as the device is not intended for these types of applications.

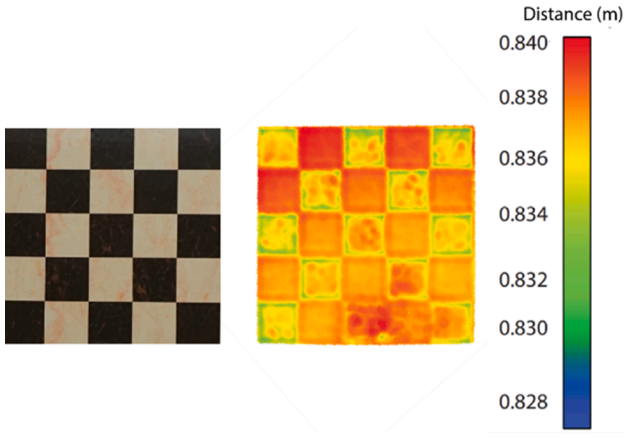

Fig. 9. Measured distance by Kinect One.

The Sony Alpha camera is able to detect the gap between the central hole and the outer frame, but could not correctly determine the magnitude of this distance. It presents high relative errors except for the depth of 1.4 mm. This is because the software assigned depth values between one and two millimeters for all the holes, hitting this measurement by chance. The lack of texture clearly makes the reconstruction by photogrammetry difficult and the error was high.

The Kinect One offers the best results in this test with relative errors lower than 20%. LIDAR technology is clearly superior on this type of surfaces with homogeneous optical properties. The intensity of the reflected light is the same in all parts of the surface and the sensor obtains the point cloud very efficiently.

Fig. 11 shows the results for the dent detection test. This test is very similar to the previous one, but represents a more realistic situation. Furthermore, dents make photogrammetry reconstruction even more difficult as there is no recognizable edge or discontinuity.

The ZED did not detect any warping, the results from this sensor are purely noise. The camera detects certain anomalies, but cannot quantify the magnitude of the depth. Whereas, the Kinect performs extraordinarily, as it can be appreciated in the disparity map. The values for the three dents in the map are quite similar to the value obtained with the caliper in the central part (7.0 mm, 5.2 mm and 1.4 mm, from left to right in the image). Although a reference point cloud was not obtained with which to compare the measurements of the Kinect, this agreement with the results of the caliper shows us the great capabilities of the sensor, despite being a low-cost device.

Fig. 12 shows the aircraft propeller scanning test. This last test, apart from being a specific aeronautic application, it is a tough test for the Kinect and ZED point cloud recording algorithms. The complex curvature of the propeller, with hardly any edges, evaluates the capacity of the cloud fusion algorithms. In general, the ZED reconstructs the scene correctly, although it obtains deviations of up to two centimeters. A truly reasonable value, given the low precision of the sensor. Kinect One, presents a good behavior in general, with deviations of a couple of millimeters for most of the blade. However, the area with black coating, near the junction of the blade with the shaft, exhibits a large deviation of up to two centimeters. The large difference in reflectivity in this region, together with the pronounced curvature, spoils the results obtained.

The Sony Alpha camera obtains the smallest deviations of the three sensors, on the order of a millimeter in almost the entire propeller. However, the reconstruction failed in the area marked in red by the disparity map. The photogrammetry software could not correctly recognize the images in this non-textured area. The main disadvantage of not performing the reconstruction in real time is that the software does not know the position from which the different photographs have

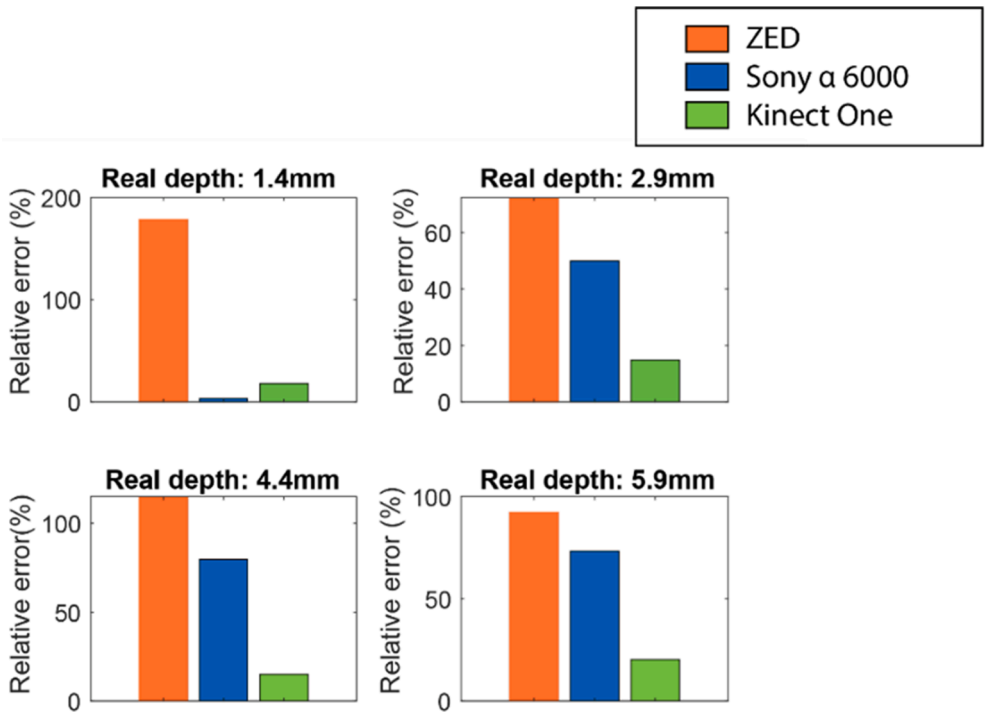

Fig. 10. Depth pattern.

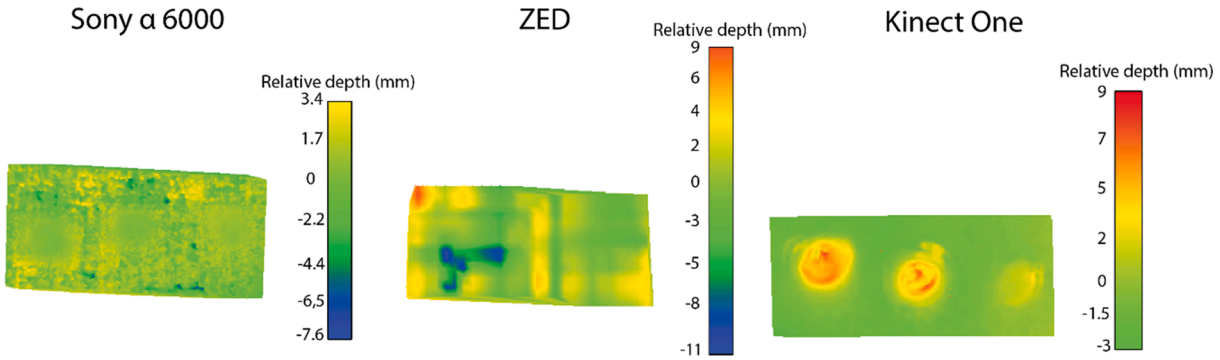

Fig. 11. Dent detection test.

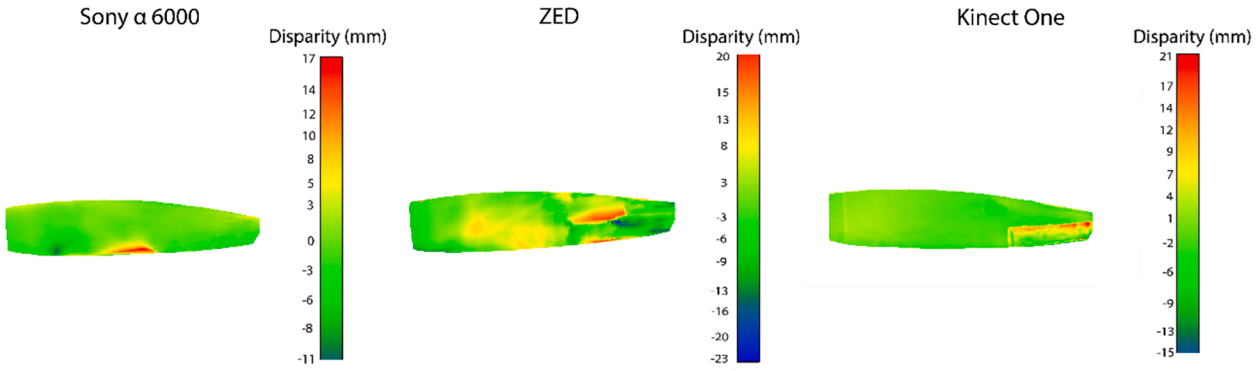

Fig. 12. Disparity map of the airplane propeller.

been obtained. On large areas without texture, this can be truly problematic, as the image identification algorithms may not be able to correctly locate the photographs. This problem could be aggravated when trying to scan large areas of airframes

Although the size of the propeller is not too big (it measures 1.35 m), a 50 mm focal length was used from about a meter of distance. Therefore, it was necessary to take a lot of pictures of the propeller. Some of them only captured the non-textured part of the blade and the software

had trouble processing them. To improve the results of this reconstruction, the focal length of the objective could be reduced, or also, the pictures could be taken from a greater distance, calibrating the camera for that range. However, although the obtained results are not satisfactory, they clearly show this problem associated to large areas without texture. Furthermore, the fact of obtaining the reconstruction through post-processing is clearly inefficient in case any error in the measurement occurs. What would mean to retake the photographs and perform the post-processing again, increasing the inspection time and costs.

4. Conclusions

Laser scanning and photogrammetric technology show potential to the inspection of aeronautical surfaces such as the fuselage or the propeller of an aircraft. However, the lack of texture in some cases makes difficult the scan process. LIDAR technology performed very well on surfaces with uniform optical properties. However, it presented a few problems in materials with poor reflectivity values. In this study, it was demonstrated how LIDAR technology could be a good candidate to scan certain parts of the fuselage, since it is a totally homogeneous surface with good reflectivity properties.

With the current scanning technologies, very good reconstruction accuracies can be obtained, with errors less than one millimeter, especially with LIDAR sensors. The Kinect One, was able to detect and quantify deformations of the order of a millimeter in the tests carried out, which is remarkable considering its low price. It is a clear indicator of the potential that LIDAR technology has on homogeneous surfaces without texture.

These results are obtained under certain laboratory conditions, in the absence of environmental errors and using post-processing techniques. In order to extend the three-dimensional scanning technology for aeronautical inspection, it is necessary ensure a high reliability and robustness against external disturbances. In addition, future trends could integrate the capabilities of unmanned aircraft systems to move the 3D scanners around the fuselage.

Declaration of Competing Interest

The authors declare that they have no known competing financial interests or personal relationships that could have appeared to influence the work reported in this paper.

Acknowledgements

Authors would like to thank the Infrastructure Technician from the School of Aerospace Engineering, Ramón Meijón, for the support given during the experimental works.

References

[1] Z. Li, D. Zhang, C. Peng, C. Ma, J. Zhang, Z. Hu, J. Zhang, Y. Zhao, The effect of local dents on the residual ultimate strength of 2024–T3 aluminum alloy plate used in aircraft under axial tension tests, Eng. Fail. Anal. 48 (2015) 21–29.
[2] M. Mydinmeera, Bird-strike aircraft accidents and their prevention, Asian J. Sci. Technol. 10 (01) (2019) 9251–9257.
[3] K. Khagendra, Aircraft and Lightning strike, Technical report, 2019.
[4] L. Shengze, Z. Weihua, F. Jin, Z. Men, Research of hail impact on aircraft Wheel door with lattice hybrid structure, J. Phys. Conf. Ser. 744 (1) (2016).
[5] Federal Aviation Agency (FAA). General operating flight rules (Code of Federal regulations, (Section 91.409).
[6] R.O. Gordon, Visual inspection for aircraft, Advisory Circular FAA (1997).
[7] Federal Aviation Agency (FAA), Aircraft inspection for the general aviation aircraft owner (1997).
[8] Airbus SAS, Airbus Innovation takes aircraft visual inspections to new heights. https://www.airbus.com/newsroom/news/en/2018/04/innovation-takes-aircraft-visual-inspections-to-new-heights.html. L. Miranda, D. Paez, Three-Dimensional Laser Scanning Test in Aircraft Surfaces, Universidad de los Andes, Colombia (2015).
[9] P. Hong-Seok, U. Mani-Tuladhar, Development of an Inspection system for defect detection in pressed parts using laser scanned data, Procedia Eng. 69 (2014) 931–936.
[10] T. Shyr, Y. Pan, Impact resistance and damage characteristics of composite laminates, Compos. Struct. 62 (2) (2003) 193–203.
[11] G.A.O. Davies, X. Zhang, Impact damage prediction in carbon composite structures, Int. J. Impact Eng. 16 (1) (1995) 149–170.
[12] D. Erchart, L.T. Ostrom, C.A. Wilhelmsen, Visual Detectibility of dents on a Composite Aircraft Inspection Specimen: An Initial Study, Int. J. Appl. Aviation Stud. 4 (2) (2004) 111–122.
[13] J. Das, D.C. Murmann, K. Cohrn, R. Raskar, A method for rapid 3D scanning and replication of large paleontological specimens, PLoS ONE 12 (7) (2017).
[14] C.S. Bamji, P. O'Connor, T.A. Elkhatib, A 0.13μm CMOS System-on-Chip for a 512 × 424 Time-of-Flight Image Sensor With Multi-Frequency Photo-Demodulation up to 130 MHz and 2GS/sAD, IEEE J. Solid-State Circ. 50 (1) (2015) 303–319.
[15] L.E. Ortiz, E.V. Cabrera, L.M. Gonçalves, Depth Data Error Modeling of the ZED 3D Vision Sensor from Stereolabs, Electron. Lett. Comput. Vision Image Analysis 17 (1) (2018) 1–15.
[16] P. Moulon, Positionnement robuste et précis de réseaux d'images, Traitement du signal et del'image, Université Paris-Est, 2014.
[17] P. Sapirstein, A high-precision photogrammetric recording system for small artifacts, J. Cult. Heritage 31 (2018) 33–35.
[18] F. Remondino, C. Fraser, Digital Camera calibration methods: considerations and comparisons, Int. Arch. Photogramm. Remote Sens. Spatial Inf. Sci. 36 (5) (2006) 266–272.
[19] C. Fraser, Digital camera self-calibration, ISPRS J. Photogramm. Remote Sens. 52 (4) (1997) 149–159.
[20] ISO 10360-4:2000, Geometrical Product Specifications (GPS) - Acceptance and reverification tests for coordinate measuring machines (CMM).
[21] OpenCV. Camera Calibration and 3D Reconstruction. https://docs.opencv.org/2.4/modules/calib3d/doc/camera_calibration_and_3d reconstruction.html.
[22] D. Brown, Close-Range Camera Calibration, DBA Systems Inc., The American Society of Photogrammetry, 1971.
[23] S. Giancola, M. Valenti, R. Sala. A Survey on 3D cameras: Metrological Comparison of Time-of-Flight, Structured-Light and Active Stereoscopy Technologies, Springer Briefs in Computer Science (2018).
[24] E. Lachat, H. Macher, M.A. Mittet, T. Landes, P. Grussenmeyer, First experiences with kinect V2 sensor for close range 3D modelling, ISPRS Int. Arch. Photogramm. Remote Sens. Spatial Inf. Sci. XL-5/W4 (2015) 93–100.
[25] H. Hirschmüller, Accurate and efficient stereo processing by semi-global matching and mutual information. IEEE Computer Society Conference on Computer Vision and Pattern Recognition (CVPR'05), 2015.
[26] Q. Chang, T. Maruyama, Real-Time Stereo Vision System: A Multi-Block Matching on GPU, 1–1, IEEE Access 6 (2018), https://doi.org/10.1109/ACCESS.2018.2859445.
[27] S. Pillai, S. Ramalingam, J.J. Leonard, High-Performance and Tunable Stereo Reconstruction. IEEE International Conference on Robotics and Automation (ICRA), 2015.